Original Article

Stomatin plays a suppressor role in non-small cell lung cancer metastasis

Huaying An[1], Xiao Ma[1], Mingyi Liu[1], Xiaotong Wang[1], Xundong Wei[2], Wei Yuan[1], Jie Ma[2]

[1]State Key Laboratory of Molecular Oncology, National Cancer Center/National Clinical Research Center for Cancer/Cancer Hospital, Chinese Academy of Medical Sciences and Peking Union Medical College, Beijing 100021, China; [2]Center of Biotherapy, Beijing Hospital, National Center of Gerontology; Institute of Geriatric Medicine, Chinese Academy of Medical Sciences, Beijing 100730, China

Correspondence to: Wei Yuan, PhD. State Key Laboratory of Molecular Oncology, Cancer Hospital, Chinese Academy of Medical Sciences and Peking Union Medical College, No. 17 Panjiayuan Nanli, Beijing 100021, China. Email: yuanwei@cicams.ac.cn; Jie Ma, PhD. Center of Biotherapy, Beijing Hospital, National Center of Gerontology; Institute of Geriatric Medicine, Chinese Academy of Medical Sciences, No. 1 Dongdan Dahua Road, Beijing 100730, China. Email: majie4685@bjhmoh.cn.

Abstract

Objective: Metastasis is one of the key causes of high mortality in lung cancer. Aberrant DNA methylation is a common event in metastatic lung cancer. We aimed to identify new epigenetic regulation of metastasis-associated genes and characterize their effects on lung cancer progression.

Methods: We screened genes associated with non-small cell lung cancer (NSCLC) metastasis by integrating datasets from the Gene Expression Omnibus (GEO) database. We obtained epigenetic-regulated candidate genes by analyzing the expression profile of demethylation genes. By overlapping analysis, epigenetically modulated metastasis-associated genes were obtained. Kaplan-Meier plotter (KM plotter) was utilized to assess the overall survival (OS) of stomatin in lung cancer. Immunohistochemistry (IHC) was conducted to determine the association between stomatin and metastasis-associated clinical indicators. Both *in vitro* and *in vivo* assays were performed to investigate the potential role of stomatin in metastasis. The regulation mechanisms of transforming growth factor β1 (TGFβ1) on stomatin were determined by Sequenom MassARRAY quantitative methylation and western blot assays.

Results: A series of bioinformatic analyses revealed stomatin as the metastasis-associated gene regulated by DNA methylation. The KM plotter analysis showed a positive association between stomatin and the OS of lung cancer. IHC analysis indicated that the decreased stomatin expression is linked with advanced TNM stage. Loss- and gain-of-function experiments displayed that stomatin could inhibit the migration and invasion of NSCLC cells. Furthermore, TGFβ1 repressed stomatin expression during epithelial-to-mesenchymal transition (EMT). The negative correlation between stomatin and TGFβ1 was also validated in advanced stage III lung tumor samples. The underlying mechanism by which TGFβ1 inhibits stomatin is due in part to DNA methylation.

Conclusions: Our results suggest that stomatin may be a target for epigenetic regulation and can be used to prevent metastatic diseases.

Keywords: Stomatin; non-small cell lung cancer; epithelial-mesenchymal transition; TGFβ1; DNA methylation

Submitted Jun 13, 2019. Accepted for publication Sep 19, 2019.
doi: 10.21147/j.issn.1000-9604.2019.06.09
View this article at: https://doi.org/10.21147/j.issn.1000-9604.2019.06.09

Introduction

Lung cancer is the most common cause of cancer-related deaths worldwide (1). Each year, the number of patients diagnosed with lung cancer is 2.1 million, with 1.8 million deaths (2,3). Despite significant advances in early diagnosis

and personalized therapy (precision medicine), the overall survival (OS) rate of lung cancer patients remains poor (5-year survival rate <15%). Metastasis is one of the key causes of poor prognosis. Therefore, it is important to identify novel key genes and their functional mechanisms to compensate for lung cancer metastasis.

DNA methylation occurs by transfer of a methyl group to a cytosine in a CpG-rich dinucleotide sequence (CpG island) by DNA methyltransferases (DNMTs) (4). Hypermethylation of gene promoter drives secondary recruitment of histone-modifying enzymes to modulate the proximate chromatin environment in lung cancer. Global genome hypomethylation can cause genomic instability, poor prognosis and overexpression of aberrant transcripts in lung cancer (5,6).

Aberrant methylation of multiple gene promoters is a common phenomenon in the key step of metastasis, epithelial-to-mesenchymal transition (EMT). Focal hypermethylation of CpG islands in EMT responsive gene promoters (e.g. *CDH1*) can be seen in various cancer cell lines and recruited with DNA methyltransferases 1 (DNMT1) by interacting with different EMT-inducing transcription factors (EMT-TFs) related to these sites (7). DNMT1 interacts with SNAI proteins through its SNAG domain (8,9) and with ZEBs through the SMAD-binding domain (10). Besides regulating the methylation state of certain genes, EMT-TFs such as *TWIST1/2* and *ZEB2* have also been modulated by DNA methylation (11,12). Transforming growth factor β (TGFβ) is the major physiologic inducer of EMT and has been utilized to stimulate EMT for analyzing epigenetic changes during cancer metastasis. TGFβ alters the activity of DNMTs to mediate global and gene specific DNA methylation and oncogenic activities (13,14). A recent bioinformatics study of TGFβ signaling pathways targeting 33 cancer types unraveled that epigenetics appears to play an important role in regulating the activity of the TGFβ superfamily pathways, especially lung adenocarcinoma (LUAD) (15). Therefore, investigating new epigenetic targets during cancer dissemination may be critical for proposing new ways to treat metastatic diseases more effectively.

Stomatin, known as human erythrocyte integral membrane protein band 7, was first purified from normal human erythrocytes to search the causes of congenital hemolytic anemia and stomatocytosis (16). The typical functions of stomatin are to control ion channels (17,18), regulate the activity of glucose transporter 1 (GLUT1) (19,20) and modulate the organization of actin cytoskeleton (21,22). A recent study suggests that stomatin clusters fusogenic assemblies to potentiate cell fusion and release membrane-bending stresses through a platform to generate forces by actin polymerization. Stomatin can be secreted into the extracellular environment by protein refolding or exosome trafficking as an enhancer of cell-fusion events (23). These findings suggest the engagement of stomatin in many biological processes. However, its potential role in cancer initiation and progression remains largely unknown.

There are few reports on the correlation between stomatin and cancer development. cDNA microarray assays showed upregulation of stomatin in diffuse-type gastric cancer (24), gastrointestinal stromal tumors (25), and colorectal cancer (26) and downregulation of stomatin in non-small cell lung cancer (NSCLC) samples (27). A recent study on human epidermal growth factor receptor 2 (HER2)-positive breast cancer indicated that decreased stomatin expression may have a poor prognosis, most likely due to a trend to distant metastases (28). In the development and progression of cancer, different gene expression depending on the type of cancer may prove important for the study of the function and mechanism of the gene. In this study, we performed an integrative analysis of two microarray datasets from the Gene Expression Omnibus (GEO) database to identify the gene signature associated with NSCLC metastasis. Then, we utilized Affymetrix Human Genome U133 Plus 2.0 expression array to identify upregulated genes in response to demethylation treatment in normal human bronchial epithelial (HBE) cells. We determined to investigate the function of stomatin in NSCLC metastasis based on the overlapping results between differentially expressed genes (DEGs) from GEO database analysis and upregulated genes induced by DNA demethylation treatment. Our study provides the direct evidence that stomatin plays a critical role in NSCLC metastasis, especially during TGFβ1-induced EMT, indicating that stomatin is a potential therapeutic target for preventing NSCLC metastasis.

Materials and methods

Bioinformatics

GSE27716 and GSE49644 datasets came from the GEO database. GSE27716, based on the Affymetrix GPL570 platform (HG-U133_Plus_2, Affymetrix Human Genome U133 Plus 2.0 Array), included 17 noninvasive

bronchioloalveolar carcinomas (BAC) and 23 adenocarcinomas with mixed (AC-mixed) subtype invasive LUAD. GSE49644, based on the Affymetrix GPL570 platform (HG-U133_Plus_2, Affymetrix Human Genome U133 Plus 2.0 Array), simulated EMT by culturing A549 and NCI-H358 cells in the presence of TGFβ for three weeks. After downloading the gene microarray expression profiles, the data qualities were assessed by weights, residuals, relative log expression (RLE), normalized unscaled standard errors (NUSE), RNA degradation curve, cluster analysis, and principal component analysis (PCA). The gene expression profiles were generated by applying robust multi-array average (RMA). The missing values were calculated by K-Nearest Neighbor (KNN). The differentially expressed genes were then identified using the limma package (version 3.40.6; http://www.bioconductor.org/packages/release/bioc/html/limma.html). The adjusted P values were utilized to reduce the false positive rate. The adjusted P<0.01 and |logFC|>0.4 were set as the cutoff criteria for GSE27716. The adjusted P<0.001 and |logFC|>0.8 were set as the cutoff criteria for GSE49644. Venn (http://bioinformatics.psb.ugent.be/webtools/Venn/) is an online tool for obtaining overlapping DEGs in these gene expression profiles. The venn diagrams were graphed by R software (Version 3.6.0; R Foundation for Statistical Computing, Vienna, Austria).

The prognostic value of stomatin in lung cancer (n=1,926), LUAD (n=720) and lung squamous cell carcinoma (LUSC) (n=524) was retrieved from the online survival analysis tool Kaplan-Meier plotter (KM plotter) database. The valid Affymetrix ID is 201061_s_at (*STOM*). A log rank P<0.05 was considered statistically significant.

The presence of CpG islands in the upstream region from +178 to −3,000 bp of stomatin gene was analyzed using EMBOSS CpGplot (http://www.ebi.ac.uk/emboss/cpgplot).

Cell lines

Cell lines were purchased from the cell culture center at Chinese Academy of Medical Sciences and Peking Union Medical College. All cells were grown at 37 ℃ in a humidified atmosphere containing 5% CO_2. HBE and H1299 cells were grown in RPMI-1640 medium (Sigma-Aldrich, St. Louis, USA, #R8758) supplemented with 10% fetal bovine serum (FBS) (Sigma, St. Louis, USA, #F3885). A549 cells were grown in the F12K Kaighn's modification medium (Gibco, Thermo Fisher Scientific, Waltham, USA, #21127022) supplemented with 10% FBS. Panc-1 cells were grown in DMEM medium (Sigma-Aldrich, #D5796) supplemented with 10% FBS. MD-MBA-231 cells were grown in L-15 medium (HyClone, GE Healthcare Life Sciences, Pittsburgh, USA, #SH30525.01) supplemented with 10% FBS.

Reagents

Recombinant human TGFβ1 protein (R&D systems, Minneapolis, USA, #240-B-002) was prepared as a stock solution of 20 μg/mL in sterile 4 mmol/L HCl containing 1 mg/mL bovine serum albumin. 5-Aza-2'-deoxycytidine (5-Aza) (Sigma-Aldrich, #A3656) was dissolved in dimethyl sulfoxide (DMSO) as a 10 mmol/L stock solution. Cycloheximide (#508739) and actinomycin D (#114666) were purchased from Sigma-Aldrich (St. Louis, USA).

Expression Profiling

Gene expression profiles between HBE and 5-Aza-treated HBE cells were compared using Human Genome U133 Plus 2.0 (Affymetrix, Thermo Fisher Scientific). Arrays were background-corrected, quantile-normalized and log-transformed.

Plasmids and RNA interference

Stomatin full-length sequence was ligated into lentivirus Ubi-MCS-3FLAG-SV40-EGFP-IRES-puromycin (GV358) (Genechem, Shanghai, China) for the overexpression of stomatin in NSCLC cell lines.

Three non-overlapping siRNAs against human stomatin were purchased from Ribobio (Ribobio, Guangzhou, China). The stomatin siRNA sequences were as follows:

si-h-STOM_001: 5'-GCACUGACAGCUUCAUCAA-3'; 3'-CGUGACUGUCGAAGUAGUU-5'. si-h-STOM_002: 5'-GGAAUGUUCUGGGCACCAA-3'; 3'-CCUUACAAGACCCGUGGUU-5'. si-h-STOM_003: 5'-GGUGGAGCGUGUGGAAAUU-3'; 3'-CCACCUCGCACACCUUUAA-5'.

In vitro cell behavior assays

Migration and invasion assays were performed using Transwell chambers with a polycarbonate nucleopore membrane (Corning, New York, USA) and BioCoat Matrigel invasion chambers (Corning, New York, USA), respectively. Indicated numbers of cells in 200 μL of FBS-free medium were seeded onto the upper chambers. The

lower compartment was filled with 500 μL of the complete medium supplemented with 10% FBS. After incubation for 24 h at 37 °C, non-migrating cells on the upper surface of the filter were removed with a cotton swab, and the migrated cells on the lower surface of the filter were fixed and stained with crystal violet solution. Five random microscopic fields were counted per field for each group, and these experiments were repeated three times independently.

Immunoblotting and antibodies

Western blot was performed to detect the expression of stomatin (abcam, Cambridge, UK, #ab169524), DNMT3A (abcam, #ab188470), E-cadherin (Cell Signaling Technology, Danvers, USA, #3195T), Slug (Cell Signaling Technology, #9585P), Claudin 1 (Cell Signaling Technology, #13255P), Vimentin (Santa Cruz Biotechnology, Dallas, USA, #sc-6260), N-cadherin (BD, Franklin Lakes, USA, #610921), β-actin (Sigma-Aldrich, #A5441).

Animal experiments

Female BALB/c-nu mice (4–5 weeks, 18–20 g) were obtained from Beijing Huafukang Bioscience (Beijing, China). All procedures were conducted in accordance with the guidelines approved by the Institutional Animal Care and Use Committee of Cancer Hospital, Chinese Academy of Medical Sciences.

A total of 3×10^6 A549-NC or A549-STOM cells per mouse in 150 μL sterile PBS were injected into the tail vein of BALB/c-nu mice. After 60 d, metastatic nodules in the lungs of the A549-NC group and A549-STOM group were observed. After lung resection, tissues were embedded in paraffin and subjected to hematoxylin-eosin (H&E) staining.

Immunofluorescence staining

Cells were seeded on microscope cover glass (Thermo Fisher Scientific, #12-545-82) in 24-well plates and fixed in 4% paraformaldehyde. Cells were stained with stomatin (abcam, #ab169524), E-cadherin (Cell Signaling Technology, #14472S), Vimentin (Santa Cruz Biotechnology, #sc-6260) and secondary Alexa Flour 488 (#A11001) or 594 (#A11012) (Life Technologies, Thermo Fisher Scientific, Waltham, USA). Images were captured by laser scanning confocal microscope (Leica, Wetzlar, Hesse, Germany) and figures were prepared under identical acquisition settings. F-actin filaments were stained with Phalloidin-iFluor 555 Reagent (abcam, #ab176756), mounted with the ProLong Gold Antifade Mountant with DAPI (Life Technologies, Thermo Fisher Scientific, #P36931) and then examined by laser scanning confocal microscope.

Immunohistochemistry and tissue microarray analysis

The lung cancer tissue microarray slides included 69 cases of LUAD with detailed information of each patient were purchased from Shanghai Outdo Biotech Co., Ltd. Immunohistochemistry of these slides was performed using antibodies, such as TGFβ1 (abcam, #ab215715) and stomatin (Proteintech, Rosemont, USA, #12046-1-AP). Tissue sections were quantitatively scored by staining intensity (range, 0–3) and the percentage of positive cells (range, 0–100%). The proportions were multiplied by 100 and then multiplied staining intensity (range, 0–300). The associations between stomatin and metastasis-associated clinical indicators, TNM stage and lymph node metastasis, were analyzed by χ^2 test. The correlation between stomatin and TGFβ1 was analyzed in LUAD samples by Spearman's rank correlation test.

Immunostaining was independently scored by two pathologists. Both of them were blinded to the patients' clinicopathological parameters. For those inconsistent scores, another pathologist was invited to reassess the staining of these tissues, and consensus scores were used for further analysis.

RNA extraction and real-time polymerase chain reaction (PCR) analysis

Total RNA was extracted using TRIzol reagent (Invitrogen, Thermo Fisher Scientific), and 500 ng of total RNA was reversely transcribed using reverse transcription reagents (Takara, Japan) as the manufacturer instructed. Real-time PCR was performed using SYBR Premix Ex Taq (Takara, Japan) on ViiA™ 7 Real-Time PCR System (Applied Biosystems). Real-time PCR primers were listed in *Supplementary Table S1*.

Sequenom MassARRAY quantitative methylation analysis

The methylation status of Stomatin promoter was detected using Sequenom MassARRAY quantitative methylation analysis platform (BGI tech, Shenzhen, China). Briefly, genomic DNA was modified by sodium bisulfite. The

target region was PCR amplified using primers labeled with T7 promoter. The PCR products were transcribed into RNA by T7 RNA polymerase, and then the RNA fragments were cleaved by base-specific RNase A to generate small fragments containing CpG sites. The generated fragments were subsequently subjected to matrix-assisted laser desorption ionization time-of-flight mass spectrometry. The signal amplitudes reflect relative fragment amounts and methylation levels. The mass shifts of 16 Da caused by the molecular weight difference between C and T represented C→T conversion after bisulfate treatment, and then represented the methylation level of the relative fragment (CpG unit). Primer sequences are shown as below: 5' end primer sequence: aggaagagag AGAGTTTTTAAGGTTGTGGGTATGA, 3' end primer sequence: cagtaatacgactcactatagggagaaggct CCTCAACCTCCCAAAT AACTAAAAT, 30 CpG sites were covered to quantify the methylation proportion of stomatin promoter in the indicated cells. Note that six detected CpG sites could not be identified in this assay.

Statistical analysis

Statistical significance was analyzed using IBM SPSS Statistics (Version 22.0; IBM Corp., New York, USA). Figures were drawn by Prism 5 software (GraphPad Software, Inc., LaJolla, CA, USA). Continuous variables were compared using a two-tailed Student's *t*-test. χ^2 test was used to assess the association between stomatin and clinical indicators. Spearman's rank correlation test was applied to assess statistical dependence between the two variables. A two-sided test was performed in all statistical tests and P<0.05 was considered statistically significant.

Results

Epigenetic study reveals association between stomatin and NSCLC development

To characterize the profile of aberrantly expressed genes in noninvasive *vs*. invasive NSCLC, we first comprehensively analyzed GSE27716, GSE49644 datasets from GEO database. The analysis showed that 2,172 genes were differentially expressed in noninvasive *vs*. invasive LUAD (GSE27716, *Figure 1A, B*, |logFC|>0.4, adj.P.value<0.01), and 2,513 were in A549-Ctrl *vs*. A549-EMT (GSE49644, *Figure 1C,D*, |logFC|>0.8, adj.P.value<0.001), and 2,295 were in H358-Ctrl *vs*. H358-EMT (GSE49644, *Figure 1E, F*, |logFC|>0.8, adj.P.value<0.001). Among these DEGs, 18 overlapping genes (*ABCG2*, *ANKRD29*, *BANK1*, *CD97*, *CFD*, *EMP1*, *FOXA2*, *KLF4*, *MID1IP1*, *PROSER2*, *RBPMS*, *SDPR*, *SGMS2*, *STOM*, *SYNGR4*, *THEM6*, *TMEM220*, *TOB1*) were consistently downregulated (*Figure 1G*), and 1 overlapped gene (*KDM7A*) was consistently upregulated in all datasets (*Figure 1H*).

Previous studies have shown that the significant suppression of EMT-related genes in NSCLC is attributed to DNA methylation (4), and we analyzed gene expression profile of HBE cells treated with DNA-demethylating agent 5-Aza-2'-deoxycytidine (5-Aza) (*Figure 1I*). Only 1 gene, stomatin, was obtained from overlapping upregulated genes in 5-Aza-treated HBE and metastasis-related DEGs (*Figure 1J*). Thus, we hypothesized that stomatin might have function during metastasis and progression of NSCLC.

To determine the association between stomatin and the OS of lung cancer patients, we assessed the effect of stomatin on the OS using KM plotter database (29). The valid Affymetrix ID is 201061_s_at (*STOM*). Survival curves were plotted for all lung cancer patients (n=1,926, *Figure 2A*), LUAD patients (n=720, *Figure 2B*), and LUSC patients (n=524, *Figure 2C*). Elevated stomatin expression was associated with favorable OS for all lung cancer patients [hazard ratio (HR)=0.69, 95% confidence interval (95% CI): 0.61−0.79, log rank P=1.7e−08] and LUAD patients (HR=0.49, 95% CI: 0.39−0.63, log rank P=6.7e−09). For LUSC patients, stomatin displayed no effect on patients' prognosis (HR=0.95, 95% CI: 0.75−1.20, log rank P=0.68). Collectively, these findings suggest that stomatin is closely correlated with a good prognosis in lung cancer patients, especially LUAD patients, implying its effect on lung cancer metastasis.

Ectopic expression of stomatin ameliorates NSCLC migration and invasion in vitro

To further address the effects of stomatin on metastasis, we detected the expressions of stomatin in NSCLC tissues through IHC and analyzed the correlation between stomatin and metastasis-associated clinical indicators such as TNM stage and lymphnode metastasis. χ^2 test analyses indicated that the decreased protein expression of stomatin was significantly associated with advanced TNM stage (P=0.006) (*Table 1*). Then we knocked down (named H1299-sistom and A549-sistom) and overexpressed stomatin in H1299 and A549 cell lines. The transwell

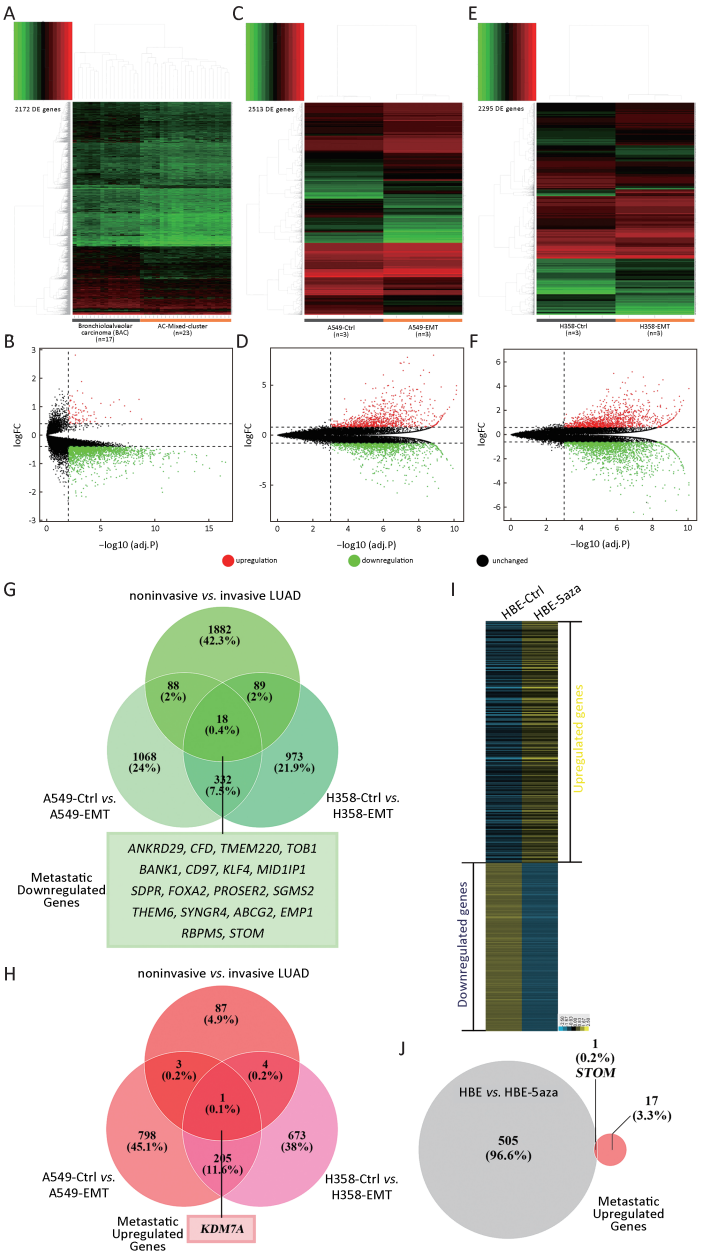

Figure 1 DEGs in non-metastatic *vs.* metastatic samples from GEO database. (A,B) Analysis of DEGs between 17 noninvasive BAC and 23 AC-mixed subtype invasive lung adenocarcinomas (GSE27716). A total of 2,172 DEGs, namely, 2,077 downregulated and 95 upregulated genes, were obtained (|logFC|>0.4; adj.P.value<0.01); (C,D) Analysis of DEGs in A549 cells before and after TGFβ1 induced EMT (GSE49644). A total of 2,513 DEGs, namely, 1,506 downregulated genes and 1,007 upregulated genes, were obtained (|logFC|>0.8; adj.P.value<0.001); (E,F) Analysis of DEGs in H358 cells with or without TGFβ1 treatment (GSE49644). A total of 2,295 DEGs, namely, 1,412 downregulated genes and 883 upregulated genes, were obtained (|logFC|>0.8; adj.P.value<0.001). The analysis results of DEGs are presented as heatmaps and volcano plots; (G,H) Venn diagrams showing upregulated (H) and downregulated (G) genes whose dysregulated expression pattern was shared by two GEO microarray database; (I) Analysis of DEGs between HBE-Ctrl and HBE-5Aza cells. HBE cells were treated with 5-Aza (10 μmol/L) for 96 h, and the medium was exchanged every day; (J) Venn diagrams show overlapping genes shared by 506 upregulated genes induced by 5Aza and 18 metastatic-associated downregulated genes. DEG; differentially expressed genes; GEO; Gene Expression Omnibus; BAC; bronchioloalveolar carcinomas; AC, adenocarcinomas; TGFβ1, transforming growth factor β1; EMT, epithelial-to-mesenchymal transition; HBE, human bronchial epithelial.

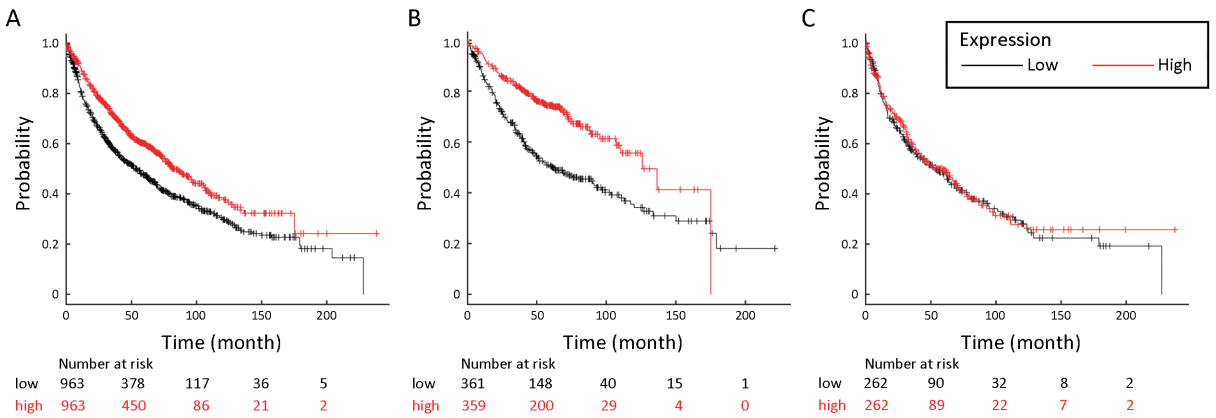

Figure 2 High expression of *STOM* is associated with better diagnosis in lung cancer, especially LUAD. Kaplan-Meier plot shows the overall survival of all lung cancer, LUAD, and LUSC patients stratified by high or low *STOM* mRNA expression (univariate Cox proportional hazards regression analysis). The valid Affymetrix ID is 201061_s_at (*STOM*). (A) Survival curve for all lung cancer patients (n=1,926), HR=0.69, 95% CI: 0.61–0.79, log rank P=1.7e–08; (B) Survival curve for LUAD (n=720), HR=0.49, 95% CI: 0.39–0.63, log rank P=6.7e–09; (C) Survival curve for LUSC (n=524), HR=0.95, 95% CI: 0.75–1.20, log rank P=0.68. LUAD, lung adenocarcinoma; LUSC, lung squamous cell carcinoma; HR, hazard ratio; 95% CI, 95% confidence interval.

Table 1 Correlation between stomatin expression and metastatic-associated clinicopathologic features (N=69)

Characteristics	Total	Stomatin expression [n (%)]		P
		Negative	Positive	
N classification				0.055
N0	42	12 (28.6)	30 (71.4)	
N1/N2/N3	25	13 (52.0)	12 (48.0)	
Nx	2	2 (100)	0 (0)	
TNM stage				0.006
I/II	53	16 (30.2)	37 (69.8)	
III	16	11 (68.8)	5 (31.3)	

migration and matrigel invasion assays were performed to investigate the biological function of stomatin in cancer metastasis. As shown in *Figure 3A–D*, the suppression of stomatin dramatically facilitated, but exogenous expression of stomatin significantly inhibited, cell migration and invasion compared to corresponding control cells.

Previous studies demonstrated the co-localization of stomatin with actin microfilaments in human amniotic epithelial cells (HAECs) and red blood cells, indicating the function of stomatin as a cytoskeletal anchor (21,22). It is well known that reorganization and reassembly of the actin cytoskeleton is critical for cancer metastasis (30,31). Thus, we did F-actin staining to characterize the effect of stomatin on actin cytoskeleton reorganization. Phalloidin staining revealed the membrane-associated actin filaments and homogeneous cytoplasmic actin in A549-sinc and H1299-sinc cells, whereas A549-sistom and H1299-sistom cells exhibited reorganization of the actin cytoskeleton with actin polymerization and formation of stress fibers (*Figure 3E*), indicating increased cellular motility.

An increase in actin stress fiber formation predicts the occurrence of EMT (32). Our GEO database analysis also indicated the downregulation of stomatin in TGFβ1-induced EMT in NSCLC cell lines. This led to examine the effect of stomatin on EMT. Exogenous stomatin expression increased, but stomatin suppression decreased, the expressions of epithelial phenotype marker (e.g., E-cadherin and Claudin 1) in A549 cells (*Figure 3F*). Meanwhile, stomatin upregulation reduced, and its downregulation induced, the mesenchymal markers' (e.g., vimentin and N-cadherin) expressions in H1299 cells (*Figure 3G*). Together, these data implied that stomatin might inhibit lung cancer metastasis in an EMT-dependent manner.

Ectopic expression of stomatin inhibits NSCLC metastasis in vivo

We injected A549-NC and A549-STOM cells (3×10^6 cells/mouse) into the tail vein of BALB/c nu/nu mice for 60 days, and visual and HE evaluation of lung metastases showed fewer and smaller foci in A549-STOM group (*Figure 4*, P=0.0265). Collectively, these results indicate that stomatin is capable of manipulating aggressive and metastatic phenotype of NSCLC both *in vitro* and *in vivo*.

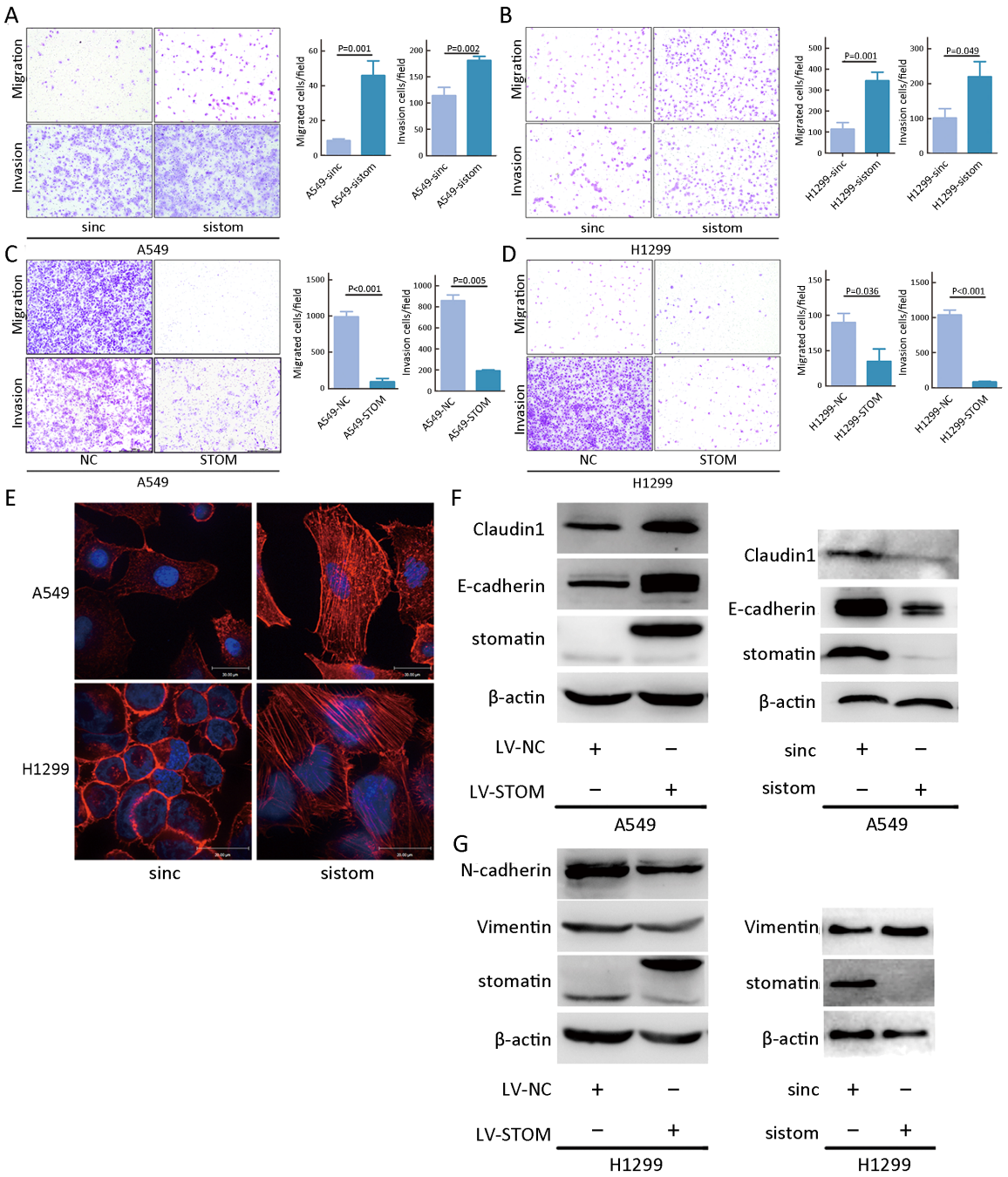

Figure 3 Stomatin can ameliorate non-small cell lung cancer (NSCLC) migration and invasion *in vitro*. (A) Cell migration (P=0.001) and invasion assays (P=0.002) of A549-sistom and corresponding control cells were performed using polycarbonate membrane transwell chambers and BioCoat Matrigel invasion chambers, respectively; (B) Results of migration (P=0.001) and invasion (P=0.049) assays of H1299-sistom and H1299-sinc; (C) Results of migration (P<0.001) and invasion (P=0.005) assays of A549-STOM and A549-NC; (D) Results of migration (P=0.036) and invasion (P<0.001) assays of H1299-STOM and H1299-NC. Representative images are shown. Magnification, ×100. The results were plotted as the average number of migrated (or invaded) cells from five random microscopic fields; (E) Phalloidin-iFlour 555 (red) was applied to characterize the effect of stomatin on cytoskeletal F-actin morphologic change in stomatin-downregulated A549 and H1299 cells. Scale bars represent 30 μm; (F) Expressions of E-cadherin and Claudin 1 in indicated cell lysates; (G) Vimentin and N-cadherin expressions in indicated cell lysates. β-actin was used as a loading control.

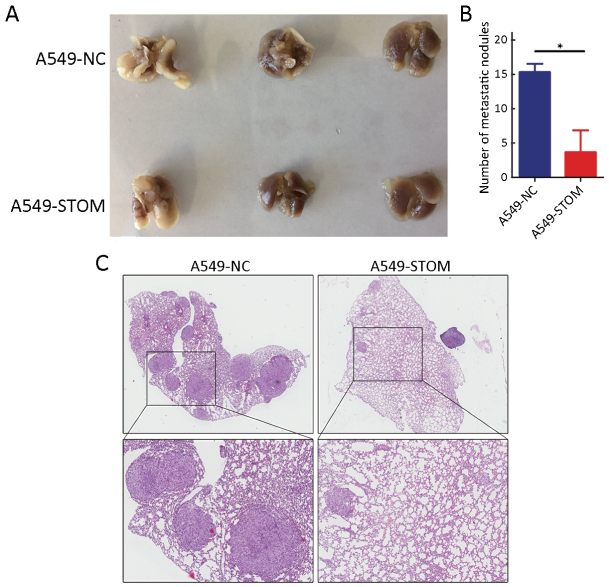

Figure 4 Stomatin inhibits non-small cell lung cancer (NSCLC) metastasis *in vivo*. (A) Representative images of visible metastatic nodules in mouse lungs of A549-NC and A549-STOM group; (B) The number of metastatic nodules in lungs was presented as $\bar{x}\pm s$ (15.33±1.202 *vs*. 3.667±3.18; *, P<0.05); (C) Representative hematoxylin and eosin (H&E) images of metastatic nodules from the mouse lung tissue sections of A549-NC and A549-STOM group (×5).

Stomatin is involved in regulation of TGFβ1-induced EMT in different types of cancer, especially in NSCLC

To explore the effects of stomatin on EMT and EMT-related gene expression, we treated A549 cell lines with TGFβ1, a major inducer of EMT. As expected, TGFβ1-treated A549 cells appeared spindle-like and exhibited fewer cell-cell interactions with decreased E-cadherin expression and increased mesenchymal markers (vimentin, N-cadherin, and slug) (*Figure 5A,B*), confirming the induction of EMT in A549 cells. As shown in *Figure 5B–D*, stomatin was strikingly attenuated in TGFβ1-treated A549 cells compared to corresponding control cells. To determine whether stomatin is suppressed by TGFβ1 in primary NSCLC, we examined the expressions of stomatin and TGFβ1 in serial sections of LUAD samples by IHC. A significant negative correlation was found between stomatin and TGFβ1 expression in advanced stage III (r=−0.501; P=0.048) tumors (*Figure 5E*) but not in early stage I–II (r=0.1; P=0.477) tumors (*Supplementary Figure S1E*). TGFβ1 also repressed stomatin expression in human pancreas/duct epithelioid carcinoma Panc-1 (*Supplementary Figure S1A–C*) and human breast adenocarcinoma MDA-MB-231 (*Supplementary Figure S1D*) cells. To further determine whether stomatin was essential for TGFβ1-induced EMT, we restored stomatin expression using lentivirus in A549 cells. As shown in *Figure 5F*, overexpression of stomatin markedly restored E-cadherin and N-cadherin mediated by TGFβ1 treatment. Taken together, these results indicate that stomatin is indispensable for TGFβ1-induced EMT, which further confirms the inhibitory function of stomatin on lung cancer metastasis.

TGFβ1 represses stomatin expression through a DNA methylation mechanism

To explore the mechanisms by which TGFβ1 represses stomatin expression during EMT, we first examined the effects of TGFβ1 on the stability of stomatin mRNA and protein by actinomycin D (AcD) and cycloheximide (CHX) chase experiment, respectively. No significant differences in the rates of stomatin mRNA and protein decay were observed upon the presence of TGFβ1 (*Supplementary Figure S2A,B*), indicating that TGFβ1 may suppress stomatin expression through other mechanisms instead of mechanisms influencing the mRNA or protein stability of stomatin.

Microarray analysis of HBE *vs*. HBE-5Aza indicated the upregulation of stomatin in response to 5-Aza, indicating the potential contribution of DNA methylation to stomatin expression. The differential stomatin expression identified in the microarray analysis was confirmed by real-time PCR (*Figure 6A*). Two possible CpG islands located in stomatin promoter at −768 to −223 (546 bp) and −143 to +122 (265 bp) relative to the transcription start site (TSS) were identified through EMBOSS cpgplot prediction (*Figure 6B*, http://emboss.bioinformatics.nl/cgi-bin/emboss/cpgplot). To confirm whether the stomatin promoter could be methylated, we assessed the methylation potential of the stomatin promoter from −768 bp to −223 bp in A549, HBE, and 5-Aza-treated A549 cells via Sequenom MassARRAY assays. The strategy is shown in *Figure 6C*. A549 cells displayed a significant decrease in methylation at most of the detectable stomatin CpG dinucleotides compared to HBE cells with lower stomatin expression (P<0.01) (*Figure 6D*). In addition, A549 cells treated with 5-Aza exhibited a further decrease in stomatin promoter methylation (P<0.01) (*Figure 6E*). Our data suggest that the expression of stomatin is inversely correlated to the degree

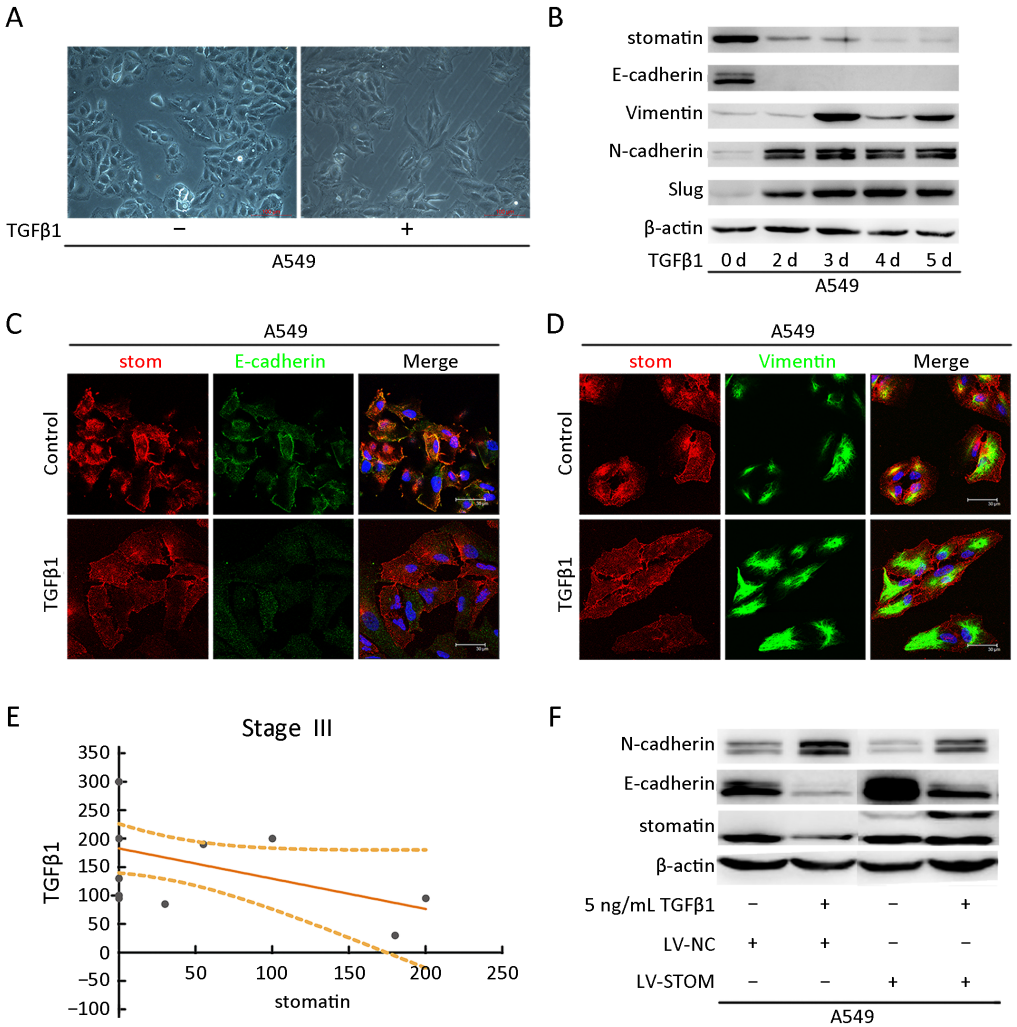

Figure 5 Stomatin is essential for transforming growth factor β1 (TGFβ1)-induced epithelial-to-mesenchymal transition (EMT) in A549 cells. (A) Representative images of TGFβ1-induced EMT in A549 cells. Scale bars represent 100 μm; (B) A549 cells were treated with 5 ng/mL TGFβ1 for indicated times, and the expressions of stomatin, E-cadherin, Vimentin, N-cadherin and Slug were assessed by western blotting. β-actin was used as a loading control; (C,D) Immunofluorescences were performed to demonstrate the inhibition of stomatin by TGFβ1. E-cadherin (C) and Vimentin (D) staining indicated the induction of EMT in A549 by TGFβ1. Scale bars represent 30 μm. (E) Semiquantitative scoring was performed on stomatin and TGFβ1 staining in lung adenocarcinoma samples. Stomatin was negatively correlated with TGFβ1 in stage III (r^2=−0.501, P=0.048) tumors; (F) A549-NC and A549-STOM cells were exposed to TGFβ1 (5 ng/mL) for 48 h. The expression levels of N-cadherin, E-cadherin, and stomatin were analyzed by western blotting. β-actin was used as a loading control.

of its DNA methylation, suggesting that TGFβ1 might silence stomatin expression through epigenetic mechanisms.

TGFβ1 induces global DNA methylation in hepatocellular tumors (33) and modulates the expression of DNA methyltransferases (DNMT1, DNMT3A, and DNMT3B), which are responsible for maintaining and establishing DNA methylation in different types of fibroblasts (34,35). A recent study on lung fibroblasts reported that TGFβ increased the expressions of both DNMT1 and DNMT3A (36). As shown in *Figure 6F*, DNMT3A protein expression was dramatically increased after 2 or 5 d of TGFβ1 treatment, and 5-Aza partly suppressed its expression.

TGFβ1-induced DNMT changes indicated methylation modification in TGFβ1-treated A549 cells. The expression

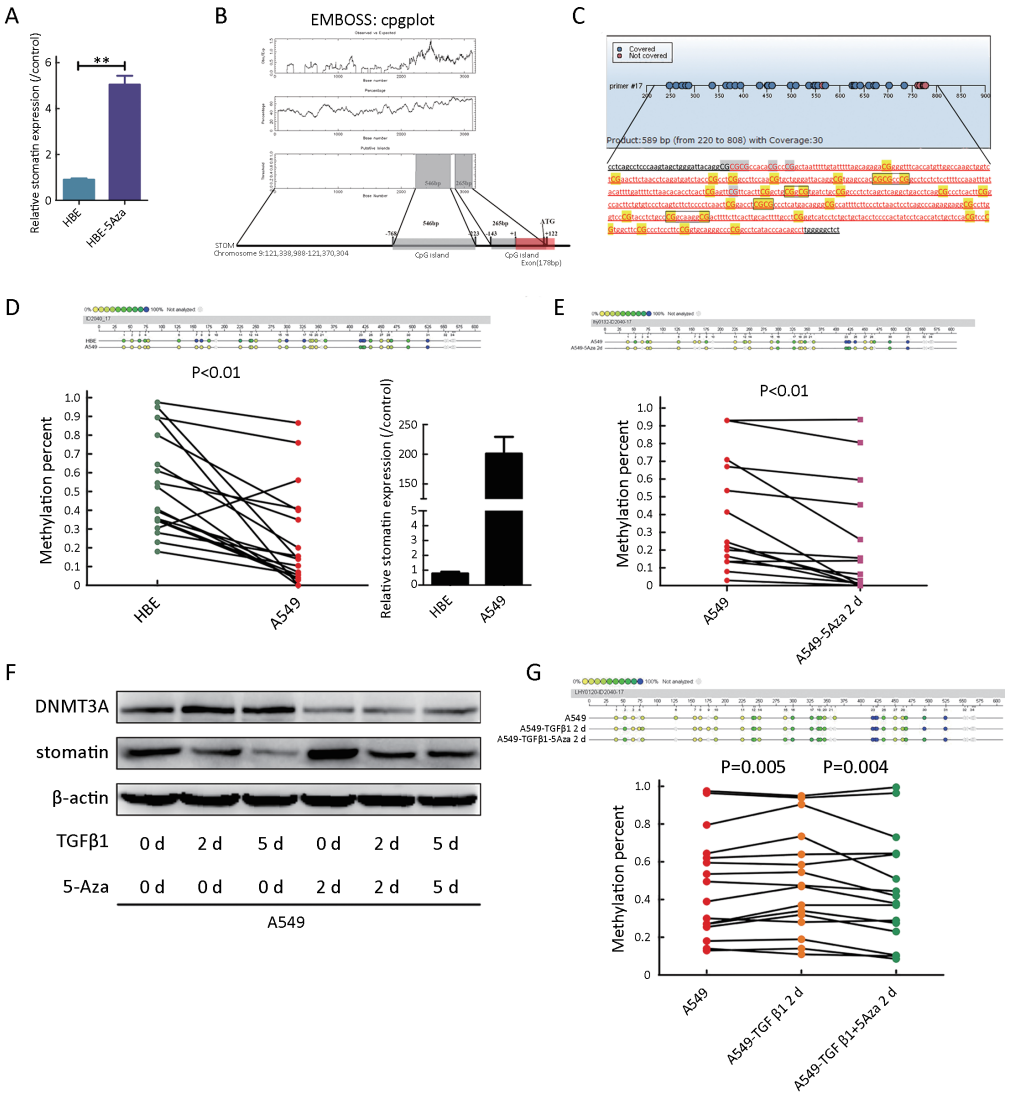

Figure 6 During transforming growth factor β1 (TGFβ1)-induced epithelial-to-mesenchymal transition (EMT), stomatin was downregulated through methylation-dependent transcription mechanism. (A) Real-time polymerase chain reaction (PCR) was performed to validate the transcriptional change of stomatin identified in the microarray. **, P<0.001; (B) Two CpG islands spanning from −768 to −223 bp and from −143 to +122 bp upstream of *STOM* gene were identified by EMBOSS cpgplot program (upper). Schematic representation of −768/−223 and −143/+122 (marked with the grey square) CpG islands in the upstream of stomatin gene (lower). Red box marked the exon. The translation start site was position +1; (C) Measuring stomatin promoter methylation levels by Sequenom MassARRAY assay; (D) Sequenom MassARRAY analysis of methylation percentages of CpG sites at the stomatin promoter. The top panel showed the methylation percentages of 30 sites in human bronchial epithelial (HBE) and A549 cells. Dots with different color depths represent different methylation status. Dark dots represent high degrees of methylation. Light dots represent low degrees of methylation. The methylation percentages of 30 CpG sites were compared by two-tailed paired Student's *t* test. In line graph, each dot represents an individual CpG dinucleotide. Green dots represent CpG dinucleotides in HBE cells. Red dots represent CpG sites in A549 cells. The corresponding detection sites were connected in a straight line. Real-time PCR was performed to evaluate the expression of stomatin in HBE and A549 cells (P<0.01); (E) The same sequenom MassArray and statistical analyses were also implemented to assess the methylation status of the indicated promoter region of stomatin in A549 and A549-5Aza cells (P<0.01); (F) A549 cells were exposed to TGFβ1 (5 ng/mL) for 2 d or 5 d with or without 5-Aza. Expression of DNMT3A and stomatin was analyzed by western blotting. β-actin was used as a loading control; (G) Sequenom MassArray analysis was implemented to assess the stomatin promoter methylation levels in A549, A549-TGFβ1, and A549-TGFβ1/5-Aza cells (P=0.005, P=0.004, respectively).

of stomatin and EMT markers was analyzed in TGFβ1-treated A549 cells with or without 5-Aza treatment. As expected, E-cadherin regulated by DNA methylation (13) was dramatically increased in response to 5-Aza, and 5-Aza restored TGFβ1-induced suppression of E-cadherin in A549 cells (*Supplementary Figure S2C*). Similarly, TGFβ1-inhibited expression of stomatin was also dramatically restored by the presence of 5-Aza (*Figure 6F*, *Supplementary Figure S2C*).

To directly verify the epigenetic regulation of stomatin in response to TGFβ1, the methylation percentage of the indicated stomatin promoter region was analyzed by Sequenom MassARRAY assays. We found that A549-TGFβ1 cells displayed a significant increase in the degree of methylation at most of CpG dinucleotides (P=0.005), whereas 5-Aza remarkably decreased the methylation percentages of these CpG sites stimulated by TGFβ1 (P=0.004, *Figure 6G*). The degree of DNA methylation of these CpG sites in response to TGFβ1 was negatively correlated with the expressions of stomatin. These results revealed that TGFβ1 suppressed stomatin by regulating its promoter DNA methylation via DNMTs.

Discussion

During the development of malignant cancer, carcinoma cells convert, at least transiently, from a fully differentiated epithelial phenotype to a dedifferentiated mesenchymal phenotype. This conversation can be enabled by activating EMT. The induction of EMT is frequently caused by epigenetic regulation. DNA methylation is a major epigenetic rule repressing gene activity and maintaining genome stability (37). DNMTs regulate DNA methylation, and overexpression of DNMTs predicts poor prognosis in lung cancer. Induction of DNMT1 or DNMT3a leads to gene silencing of tumor suppressor genes (TSGs) such as *CDKN2A, FHIT, RARβ*, by DNA hypermethylation. DNA methyltransferase inhibitors (DNMTi) are extensively studied as a powerful therapeutic agent in lung cancer (6). A subset of epigenetically regulated genes is associated with EMT processes in NSCLC, and many genes that distinguish "epithelial-like" cells from "mesenchymal-like" cells are downregulated by DNA methylation during the EMT process (38).

Considering the frequent occurrence of DNA methylation during cancer metastasis, we integrated noninvasive *vs*. invasive adenocarcinoma (AC) tumor dataset and TGFβ1-induced EMT NSCLC cell line dataset, and identified 18 downregulated and 1 upregulated candidate genes associated with NSCLC metastasis. Then, we analyzed the expression profile of 5-Aza treated and untreated HBE cells to determine the candidate genes regulated by DNA methylation. By overlapping analysis, we obtained a new metastasis-associated methylation-regulated gene, stomatin. The online KM plotter database analysis of stomatin indicated its favorable effect on LUAD OS survival. IHC staining of LUAD tissues further confirmed the correlation between stomatin and TNM stage. The following function studies have showed that stomatin inhibited the migration and invasion of NSCLC cells and suppressed the occurrence of EMT. And its expression was repressed during TGFβ1-induced EMT. Through promoter CpG island prediction and Sequenom MassARRAY analysis, we verified the regulation of stomatin expression by DNA methylation. These evidences confirmed that stomatin is associated with metastasis and DNA methylation.

To directly confirm the epigenetic regulation of stomatin expression in response to TGFβ1, we analyzed the stomatin promoter methylation status by Sequenom MassARRAY analysis. This assay is one of the first high-throughput and quantitative DNA methylation methods. It analyzes bisulfate converted DNA through base-specific cleavage of nucleotides and subsequent MALDI-TOF MS fragment analysis. The methylation values are highly accurate, and the method is very reproducible (39,40). The methylation percentages of the stomatin promoter CpG dinucleotide sites displayed an increased tendency in response to TGFβ1. More importantly, this increase could be reversed by the addition of 5-Aza. These results not only support the aforementioned concept that aberrant DNA methylation not only affects the activity of the TGFβ pathway but also highlights the modulation of stomatin expression through DNA hypomethylation during TGFβ1-induced EMT. To our knowledge, this is the first study that puts forth this concept.

However, the results of the Sequenom MassARRAY assays did not reveal any methylation alterations in pancreatic cancer cells treated with or without TGFβ1. Mechanisms other than DNA methylation may explain stomatin downregulation in TGFβ1-treated Panc-1 cells. Further research is needed to sufficiently understand the global modulation mechanisms of TGFβ1 on stomatin.

Similar to proteins that play a structural role in plasma membrane organization, stomatin is present in a higher-order oligomeric form and is associated with lipid rafts.

Stomatin typically functions as a modulator of ion channels in sensory neurons and interacts with GLUT1 to regulate cellular glucose transport in human erythrocytes. Another essential function of stomatin is to co-localize with actin microfilaments. In A549 cell lines, dex- and/or hypoxia-induced stomatin is demonstrated to stabilize the membrane-associated actin cytoskeleton. In our study, cytoplasmic actin remodeling was observed in cells lacking stomatin, which corresponds to aforementioned evidences of membrane-associated actin stabilization induced by stomatin and further supports the function of stomatin to inhibit NSCLC metastasis.

Monomeric actin is a globular ATP-ADP binding protein, and ATP-actin rapidly and almost completely polymerizes into structurally polarized filaments (F-actin). Biologically, the reorganization and assembly of the actin cytoskeleton is involved in almost all steps of metastatic spread, such as the detachment of cell-cell contacts, invadopodia and pseudopodia formation, and motility (30). In addition to the structural characteristics of actin, the dynamic properties of the actin meshwork modulated by myosin-II also regulate the recruitment of E-cadherin, thereby regulating intercellular adhesion and dissemination of cancer cells (41).

Rho family GTPases is one of the major protein families that regulate the rearrangement of the actin cytoskeleton (42). Members of this family control almost all aspects of cellular motility and invasion. Many studies have indicated that Rho GTPases regulates cell dissemination in many cancers by mediating the remodeling the actin cytoskeleton, as well as by transmitting signals from plasma membrane receptors to regulate focal adhesion, cell polarity, and vesicular trafficking (43,44). We have some preliminary results about the association between Rho GTPases and stomatin (data not shown). Combining the above findings and our previous data, we propose a potential mechanism of a stomatin-Rho-actin module in invasive lung cancer. It would be interesting to elucidate the mechanisms by which stomatin organizes and regulates actin cytoskeleton structures to impede the metastatic spread of lung cancer.

Conclusions

Our study identified a novel metastasis-associated methylation-regulated gene, *stomatin*, and uncovered its function during the metastasis of NSCLC, indicating that stomatin acts as a novel biomarker to prevent NSCLC metastasis.

Acknowledgements

This study was supported by the National Natural Science Foundation of China (No. 81602576, 81802872); National Key Research and Development Program of China (No. 2016YFA0201503); Chinese Academy of Medical Sciences Innovation Fund for Medical Sciences (CIFMS) (No. 2016-I2M-1-007, 2018-I2M-1-002).

Footnote

Conflicts of Interest: The authors have no conflicts of interest to declare.

References

1. National Health Commission of the People's Republic of China. Chinese guidelines for diagnosis and treatment of primary lung cancer 2018 (English version). Chin J Cancer Res 2019;31:1-28.
2. Bray F, Ferlay J, Soerjomataram I, et al. Global cancer statistics 2018: GLOBOCAN estimates of incidence and mortality worldwide for 36 cancers in 185 countries. CA Cancer J Clin 2018;68:394-424.
3. Liu S, Chen Q, Guo L, et al. Incidence and mortality of lung cancer in China, 2008-2012. Chin J Cancer Res 2018;30:580-7.
4. Ehrlich M. DNA hypermethylation in disease: mechanisms and clinical relevance. Epigenetics 2019; 14:1141-63.
5. Liloglou T, Bediaga NG, Brown BR, et al. Epigenetic biomarkers in lung cancer. Cancer Lett 2014;342: 200-12.
6. Mehta A, Dobersch S, Romero-Olmedo AJ, et al. Epigenetics in lung cancer diagnosis and therapy. Cancer Metastasis Rev 2015;34:229-41.
7. Skrypek N, Goossens S, De Smedt E, et al. Epithelial-to-mesenchymal transition: Epigenetic reprogramming driving cellular plasticity. Trends Genet 2017;33:943-59.
8. Lim SO, Gu JM, Kim MS, et al. Epigenetic changes induced by reactive oxygen species in hepatocellular carcinoma: methylation of the E-cadherin promoter. Gastroenterology 2008;135:2128-40,2140.e1-8.
9. Espada J, Peinado H, Lopez-Serra L, et al. Regulation

of SNAIL1 and E-cadherin function by DNMT1 in a DNA methylation-independent context. Nucleic Acids Res 2011;39:9194-205.
10. Fukagawa A, Ishii H, Miyazawa K, et al. δEF1 associates with DNMT1 and maintains DNA methylation of the E-cadherin promoter in breast cancer cells. Cancer Med 2015;4:125-35.
11. Galván JA, Helbling M, Koelzer VH, et al. TWIST1 and TWIST2 promoter methylation and protein expression in tumor stroma influence the epithelial-mesenchymal transition-like tumor budding phenotype in colorectal cancer. Oncotarget 2015; 6:874-85.
12. Li A, Omura N, Hong SM, et al. Pancreatic cancers epigenetically silence SIP1 and hypomethylate and overexpress miR-200a/200b in association with elevated circulating miR-200a and miR-200b levels. Cancer Res 2010;70:5226-37.
13. Cardenas H, Vieth E, Lee J, et al. TGF-β induces global changes in DNA methylation during the epithelial-to-mesenchymal transition in ovarian cancer cells. Epigenetics 2014;9:1461-72.
14. Suriyamurthy S, Baker D, Ten Dijke P, et al. Epigenetic reprogramming of TGF-β signaling in breast cancer. Cancers (Basel) 2019;11.pii:E726.
15. Korkut A, Zaidi S, Kanchi RS, et al. A Pan-cancer analysis reveals high-frequency genetic alterations in mediators of signaling by the TGF-β superfamily. Cell Syst 2018;7:422-37.
16. Lapatsina L, Brand J, Poole K, et al. Stomatin-domain proteins. Eur J Cell Biol 2012;91:240-5.
17. Genetet S, Desrames A, Chouali Y, et al. Stomatin modulates the activity of the Anion Exchanger 1 (AE1, SLC4A1). Sci Rep 2017;7:46170.
18. Moshourab RA, Wetzel C, Martinez-Salgado C, et al. Stomatin-domain protein interactions with acid-sensing ion channels modulate nociceptor mechano-sensitivity. J Physiol 2013;591:5555-74.
19. Montel-Hagen A, Kinet S, Manel N, et al. Erythrocyte Glut1 triggers dehydroascorbic acid uptake in mammals unable to synthesize vitamin C. Cell 2008;132:1039-48.
20. Rungaldier S, Oberwagner W, Salzer U, et al. Stomatin interacts with GLUT1/SLC2A1, band 3/SLC4A1, and aquaporin-1 in human erythrocyte membrane domains. Biochim Biophys Acta 2013; 1828:956-66.
21. Chen JC, Cai HY, Wang Y, et al. Up-regulation of stomatin expression by hypoxia and glucocorticoid stabilizes membrane-associated actin in alveolar epithelial cells. J Cell Mol Med 2013;17:863-72.
22. Rungaldier S, Umlauf E, Mairhofer M, et al. Structure-function analysis of human stomatin: A mutation study. PLoS One 2017;12:e0178646.
23. Lee JH, Hsieh CF, Liu HW, et al. Lipid raft-associated stomatin enhances cell fusion. FASEB J 2017;31:47-59.
24. Jinawath N, Furukawa Y, Nakamura Y. Identification of NOL8, a nucleolar protein containing an RNA recognition motif (RRM), which was overexpressed in diffuse-type gastric cancer. Cancer Sci 2004;95:430-5.
25. Subramanian S, West RB, Corless CL, et al. Gastrointestinal stromal tumors (GISTs) with KIT and PDGFRA mutations have distinct gene expression profiles. Oncogene 2004;23:7780-90.
26. Kwon HC, Kim SH, Roh MS, et al. Gene expression profiling in lymph node-positive and lymph node-negative colorectal cancer. Dis Colon Rectum 2004; 47:141-52.
27. Arkhipova KA, Sheyderman AN, Laktionov KK, et al. Simultaneous expression of flotillin-1, flotillin-2, stomatin and caveolin-1 in non-small cell lung cancer and soft tissue sarcomas. BMC Cancer 2014;14:100.
28. Chen CY, Yang CY, Chen YC, et al. Decreased expression of stomatin predicts poor prognosis in HER2-positive breast cancer. BMC Cancer 2016; 16:697.
29. Győrffy B, Surowiak P, Budczies J, et al. Online survival analysis software to assess the prognostic value of biomarkers using transcriptomic data in non-small-cell lung cancer. PLoS One 2013;8:e82241.
30. Nürnberg A, Kitzing T, Grosse R. Nucleating actin for invasion. Nat Rev Cancer 2011;11:177-87.
31. Gerashchenko TS, Novikov NM, Krakhmal NV, et al. Markers of cancer cell invasion: are they good enough? J Clin Med 2019;8.pii:E1092.
32. Lamouille S, Xu J, Derynck R. Molecular mechanisms of epithelial-mesenchymal transition. Nat Rev Mol Cell Biol 2014;15:178-96.
33. Martin M, Ancey PB, Cros MP, et al. Dynamic imbalance between cancer cell subpopulations induced by transforming growth factor beta (TGF-β)

is associated with a DNA methylome switch. BMC Genomics 2014;15:435.
34. Pan X, Chen Z, Huang R, et al. Transforming growth factor beta1 induces the expression of collagen type I by DNA methylation in cardiac fibroblasts. PLoS One 2013;8:e60335.
35. Neveu WA, Mills ST, Staitieh BS, et al. TGF-β1 epigenetically modifies Thy-1 expression in primary lung fibroblasts. Am J Physiol Cell Physiol 2015;309:C616-26.
36. Koh HB, Scruggs AM, Huang SK. Transforming growth factor-β1 increases DNA methyltransferase 1 and 3a expression through distinct post-transcriptional mechanisms in lung fibroblasts. J Biol Chem 2016;291:19287-98.
37. Yan F, Shen N, Pang J, et al. Restoration of miR-101 suppresses lung tumorigenesis through inhibition of DNMT3a-dependent DNA methylation. Cell Death Dis 2014;5:e1413.
38. Lin SH, Wang J, Saintigny P, et al. Genes suppressed by DNA methylation in non-small cell lung cancer reveal the epigenetics of epithelial-mesenchymal transition. BMC Genomics 2014;15:1079.
39. Ehrich M, Nelson MR, Stanssens P, et al. Quantitative high-throughput analysis of DNA methylation patterns by base-specific cleavage and mass spectrometry. Proc Natl Acad Sci U S A 2005; 102:15785-90.
40. Coolen MW, Statham AL, Gardiner-Garden M, et al. Genomic profiling of CpG methylation and allelic specificity using quantitative high-throughput mass spectrometry: critical evaluation and improvements. Nucleic Acids Res 2007;35:e119.
41. Engl W, Arasi B, Yap LL, et al. Actin dynamics modulate mechanosensitive immobilization of E-cadherin at adherens junctions. Nat Cell Biol 2014;16:587-94.
42. Thomas P, Pranatharthi A, Ross C, et al. RhoC: a fascinating journey from a cytoskeletal organizer to a Cancer stem cell therapeutic target. J Exp Clin Cancer Res 2019;38:328.
43. Hanna S, El-Sibai M. Signaling networks of Rho GTPases in cell motility. Cell Signal 2013;25: 1955-61.
44. Ridley AJ. Rho GTPase signalling in cell migration. Curr Opin Cell Biol 2015;36:103-12.

Cite this article as: An H, Ma X, Liu M, Wang X, Wei X, Yuan W, Ma J. Stomatin plays a suppressor role in non-small cell lung cancer metastasis. Chin J Cancer Res 2019;31 (6):930-944. doi: 10.21147/j.issn.1000-9604.2019.06.09

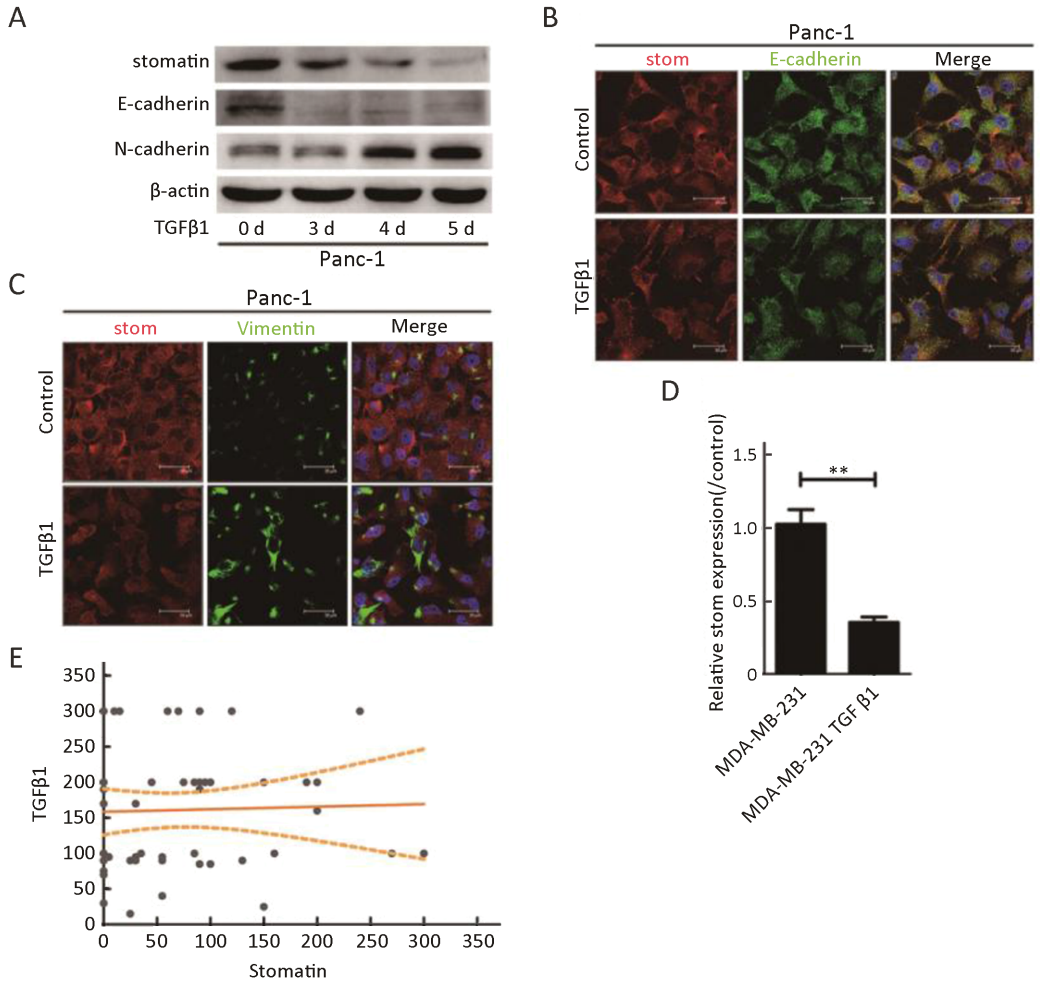

Figure S1 Stomatin is inhibited during transforming growth factor β1 (TGFβ1)-induced epithelial-to-mesenchymal transition (EMT) in Panc-1 and MDA-MB-231 cells. (A) Panc-1 cells were treated with 10 ng/mL TGFβ1 for the indicated times, and expressions of stomatin, E-cadherin, and N-cadherin were assessed by western blotting. β-actin was used as a loading control; (B,C) Immunofluorescence microscopy was performed to demonstrate the inhibition of stomatin expression by TGFβ1. E-cadherin (B) and Vimentin (C) staining indicated the induction of EMT in Panc-1 by TGFβ1. Scale bars represents 30 μm; (D) MDA-MB-231 cells were treated with 10 ng/mL TGFβ1 for 2 d, and the expression of stomatin was assessed by real-time polymerase chain reaction (PCR). *, P<0.05. **, P<0.001. Three independent experiments were performed; (E) Semiquantitative scoring was performed, and stomatin scores had no correlation with TGFβ1 scores in stage I and II (r=0.1, P=0.477, n=53) lung adenocarcinomas.

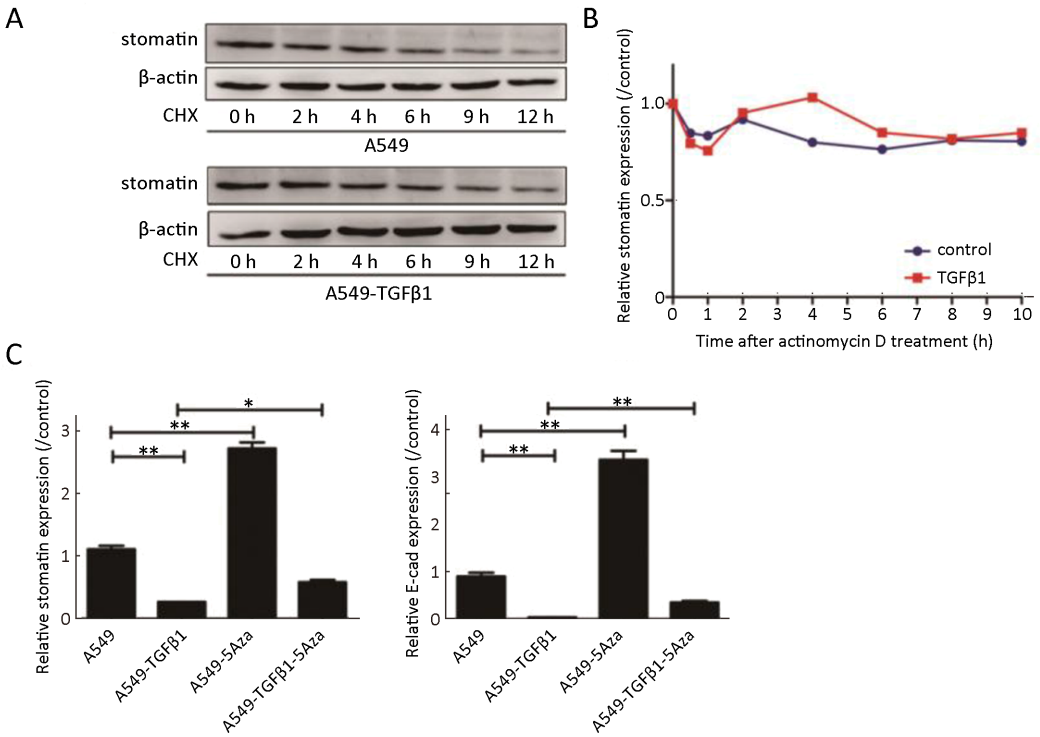

Figure S2 Mechanisms of stomatin inhibition during transforming growth factor β1 (TGFβ1)-induced epithelial-to-mesenchymal transition (EMT). (A) A549 cells were treated with or without 5 ng/mL TGFβ1. After 12 h, cells were treated with 5 μg/mL cycloheximide (CHX) for the indicated times with or without TGFβ1. Endogenous stomatin was detected by western blotting. β-actin was used as a loading control; (B) A549 cells were stimulated with 5 ng/mL TGFβ1 for 12 h before 10 μg/mL actinomycin D (AcD) treatment; the cells were incubated with AcD for the indicated times. The expression of stomatin was determined by quantitative real-time polymerase chain reaction (PCR). Three independent experiments were performed; (C) A549 cells were exposed to TGFβ1 (5 ng/mL) for 2 d with or without 5-Aza. Expressions of E-cadherin, and stomatin were analyzed by real-time PCR. *, P<0.05, **, P<0.001. Three independent experiments were performed.

Table S1 Primer sequences used for real-time PCR

Gene	Forward primer	Reverse primer
Stomatin	CACACACGGGACTCCGAAG	ATGAGAACGCCACCAAAATCC
E-cadherin	TGCCCAGAAAATGAAAAAGG	GTGTATGTGGCAATGCGTTC
β-actin	CATGTACGTTGCTATCCAGG	CTCCTTAATGTCACGCACGAT

PCR, polymerase chain reaction.

